# How to Adapt Scatchard Plot for Graphically Addressing Cooperativity in Multicomponent Self-Assemblies

**Josef Hamacek* and Claude Piguet**

*Department of Inorganic, Analytical and Applied Chemistry, University of Geneva, 30 quai E. Ansermet, CH-1211 Geneva 4, Switzerland*

*Received: November 29, 2005; In Final Form: February 23, 2006*

A graphical method has been developed for the reliable detection of cooperativity in polymetallic complexes involving intra- and intermolecular complexation processes. The method relies on the determination of the partial occupancy $r_{AL_n}$, which represents the average number of metals bound per preassembled receptor $AL_n$ made up of $n$ ligands bound to a linker A. We observe nonlinear, i.e., nonstatistical, Scatchard-like plots ($r_{AL_n}$/[M] vs $r_{AL_n}$) for metal-binding in double-stranded helicates. The present concept is extended to a virtual, pre-organized receptor $L_n$, in which no specific linker is involved. Applications to several polymetallic helicates reveal the presence of negatively cooperative processes attributed mainly to intermetallic repulsions, in agreement with recent thermodynamic models.

## Introduction

Several theoretical models have been recently developed for (i) the rationalization and interpretation of thermodynamic data and (ii) the assessment of cooperativity in supramolecular chemistry. The repetitive-binding[1] and the site-binding[2−5] models explicitly address cooperativity by using a microscopic parametrization of macroscopic formation constants. Detailed applications of this modeling to polymetallic helicates leading to some reliable assessment of cooperativity have been discussed by Piguet et al.[6] However, the conclusions derived from these thermodynamic models are usually in contrast with the results of classical, graphical cooperativity tests, which points out an inappropriate use of these tests.[1]

In biological systems, cooperativity is attributed to a behavior, where an initial binding of a ligand L to a receptor (macromolecule) induces allosteric effects, which changes the binding affinity of an identical site toward the subsequent ligand L. Positive cooperativity is evidenced by a statistically normalized enhancement of binding strength. In the opposite case, we are dealing with negative cooperativity. A detailed review of the formal aspects of cooperative binding in biology was convincingly presented by Perlmutter-Hayman.[7] Cooperativity is usually evaluated using graphical tests, such as the binding curve and the Scatchard and Hill plots. These methods for representing experimental results are all equivalent. All of them are based on the calculation of the occupancy $r$, which corresponds to the average number of ligands bound per receptor. The occupancy $r$ is obtained for a classical binding of L to a receptor P with eq 1, whereby the concentrations of the species can be easily expressed in terms of stability constants.[7]

$$r = \frac{[PL] + 2[PL_2] + ... + n[PL_n]}{[P] + [PL] + [PL_2] + ... + [PL_n]} \qquad (1)$$

Although the binding curve ($r$ as a function of [L]) and the Hill plot (log($r$/($t - r$) vs log [L], whereby $t$ accounts for the total number of equivalent binding sites within the receptor)[7] are also common tests for cooperativity, we will focus on the discussion of the Scatchard plot ($r$/[L] vs $r$),[7,8] because of its relatively simple interpretation. This plot easily evidences deviations from noncooperative, i.e., statistical, behavior related to the linear form of the binding isotherm.[1,9] A concave downward curve (concave), a straight line, and a concave upward (convex) curve respectively correspond to positive, statistical (noncooperative), and negative cooperativity. Although allosteric effects are common in biological systems (e.g., hemoglobin), cooperative ligand−receptor interactions were also reported for artificial supramolecular systems.[9] For instance, the recent self-assembly of pseudorotaxane complexes[10] represents a typical case of positively cooperative processes, for which a typical downward Scatchard plot is constructed.

In coordination chemistry, receptor−ligand interactions are replaced by ligand−metal interactions, and two different situations may occur. First, the metal center behaves as a receptor and eq 1 is easily adapted for the successive binding of ligands to a single metal ion (i.e., P = M). Extensive theoretical treatment of the associated equilibria can be found, for instance, in the seminal contribution of Ercolani.[1] The application of the Scatchard plot is adequate, which allows the assessment of cooperativity for usual monometallic coordination complexes (e.g., negative cooperativity in Ni−$NH_3$ complexes,[11] Figure 1a). The second situation arises, when the role of ligands and metal ions is inverted. The occupancy $r$ can be thus defined for the successive binding of metals to a single polytopic ligand L, which behaves as a simple receptor. These metal binding reactions are conveniently described by means of the binding partition function $Q$, which represents the sum of concentrations of all species containing L ($[L]_{tot}$) relative to some reference species, such as free [L]. Finally, $Q$ corresponds to the metal-binding (often termed M-binding) polynomial given by eq 2, whereby $\beta_m$ are the overall macroscopic binding constants.

* Corresponding author. E-mail: Josef.Hamacek@chiam.unige.ch.

10.1021/jp056932c CCC: $30.25 
Published on Web 03/25/2006

$$Q = \frac{[L]_{tot}}{[L]} = \frac{[L] + [ML] + [M_2L] + ... + [M_mL]}{[L]} = 1 + \sum_m \beta_m [M]^m \quad (2)$$

The degree of metal binding to L, which corresponds to the classical occupancy *r*, is given by eq 3 as the derivative of ln *Q* with respect to ln [M]. The detailed mathematical solution of the derivative (eq 3) can be found, for instance, in ref 12.

$$r = \frac{\partial \ln Q}{\partial \ln[M]} = \frac{\sum_m m\beta_m [M]^m}{1 + \sum_m \beta_m [M]^m} \quad (3)$$

Furthermore, eq 3 indeed corresponds to

$$r = \frac{\sum_m m\beta_m [M]^m}{1 + \sum_m \beta_m [M]^m} = \frac{[ML] + 2[M_2L] + ... + m[M_mL]}{[L] + [ML] + [M_2L] + ... + [M_mL]} = \frac{[M]_{bound}}{[L]_{tot}} = \frac{[M]_{tot} - [M]}{[L]_{tot}} \quad (4)$$

which introduces the total concentrations of reagents. This treatment can be safely applied for polymetallic complexes with a single ligand. A typical example is given by the $K^+$ complexes with the $D_2$-symmetrical ligand L1 possessing two strictly equivalent binding sites.[13] The convex Scatchard plot (Figure 1b) related to two intermolecular reactions with $K^+$ reveals negatively cooperative binding of the second $K^+$ due to the intermetallic repulsion.[13]

The ditopic tripodal ligand L2 corresponds to a more complex receptor (Scheme 1), because the two coordination cavities are different. However, assuming a pseudo-$C_2$ symmetry (i.e., the two sites are equivalent) allows the use of a standard Scatchard plot. With this approximation, positive cooperativity has been evidenced by Blanc et al. for the successive fixation of two Fe(III) to L2 (Figure 1c).[14] Generally speaking, the use of Scatchard plots for estimating cooperativity in polytopic receptors requires *n* strictly equivalent binding sites related by $C_n$ or $S_n$ symmetry axes. This is rarely met in chemistry and/or in biology, and some approximation of pseudo-$C_n$ or pseudo-$S_n$ symmetry (as shown above for L2) is commonly used for describing the successive binding of ligands to a macromolecule.

This approximation has been also applied for trimetallic double-stranded[15,16] and triple-stranded helicates,[17] and elegant downward Scatchard plots (see Figure 3a and Figure 7a) are obtained suggesting strong positive cooperativity. However, it was shown by Ercolani, that the use of the Scatchard plot and related tests for cooperativity (the binding curves, the Hill plots) is inadequate for these helicates, because the stepwise stability constants refer to virtually nonequivalent processes combining intra- and intermolecular processes.[1] Moreover, negative cooperativity for the formation of polymetallic helicates with the neutral ligands L3, L4, and L6 (Scheme 1) has been eventually evidenced thanks to a thorough analysis using the extended site-binding model.[2−5] Regarding these contrasting conclusions concerning cooperativity, an important question arises: how is it possible that the occupancy-based tests failed, i.e., the Scatchard plot provides concave downward curves when negative cooperativity operates (Figures 3a and 7a)?

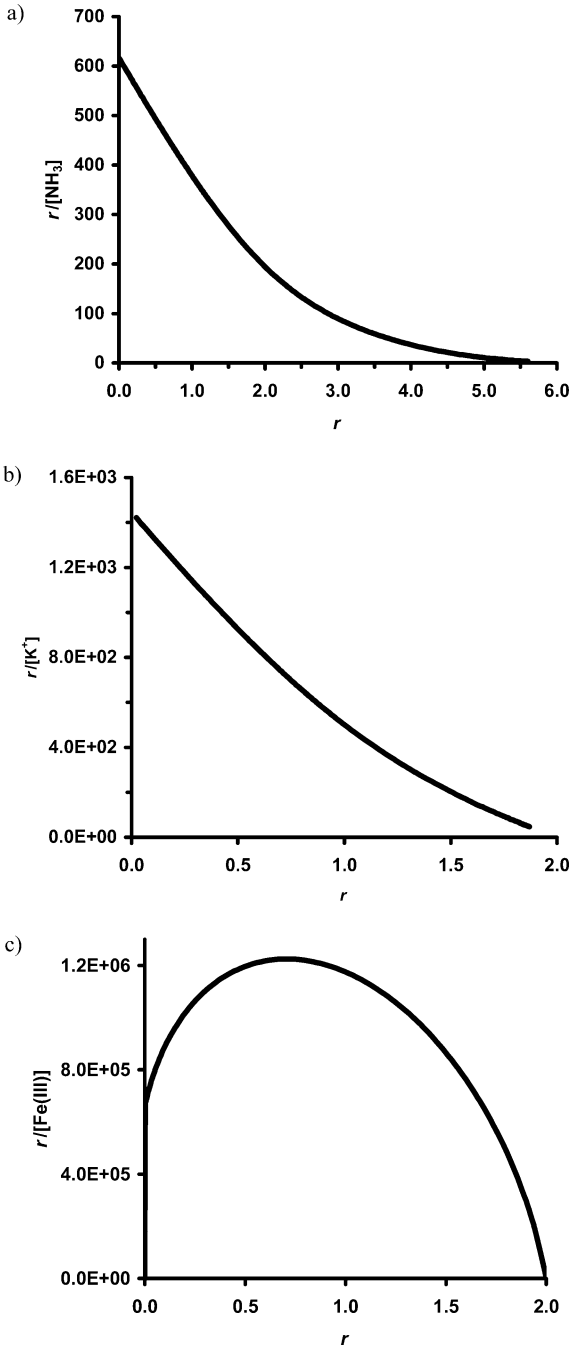


**Figure 1.** (a) Convex Scatchard plot for the formation of $[Ni(NH_3)_n]^{2+}$ ($n = 1-6$). Computed by using the stability constants reported in ref 11. (b) Convex Scatchard plot for the formation of $K^+$ complexes with L1. Computed by using the stability constants reported in ref 13 ($KPF_6$, $Me_2CO$). (c) Concave Scatchard plot for the formation of Fe(III) helicates with L2. Computed by using the stability constants reported in ref 14.

In this contribution, we reexamine the use of graphical methods, especially the Scatchard plot, for the formation of multimetallic helicates, in which intra- and intermolecular processes occur. A novel graphical plot, which operates with the partial occupancy related to a preassembled receptor, is proposed for an easy and reliable detection of cooperativity in these self-assembly processes. The application of this method

**SCHEME 1: Ligand Structures and Schematic Structures of Receptors**

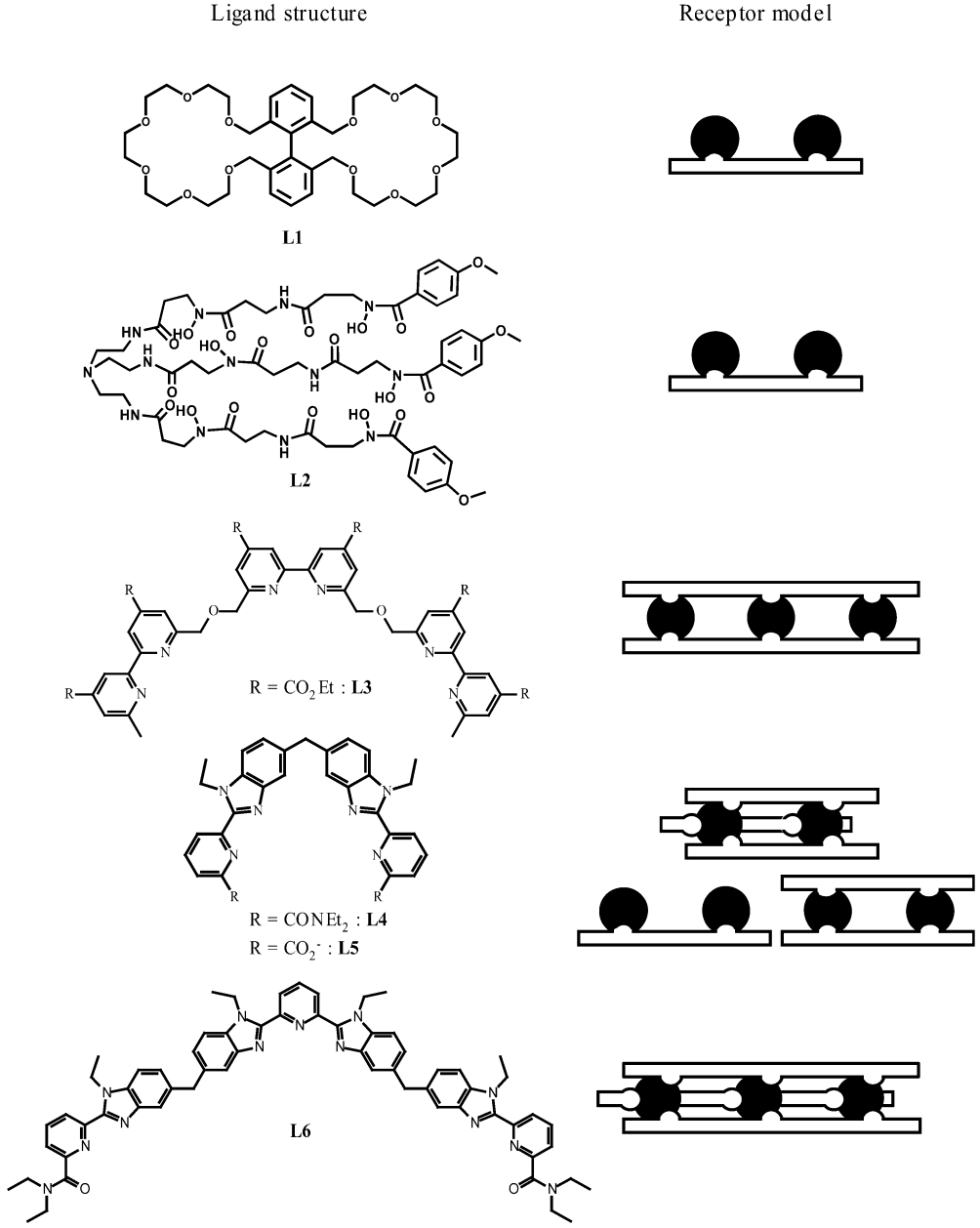


is discussed for some helicate systems, which have been previously treated with standard Scatchard plots.

## Experimental Section

**Computational Details.** Computations of concentrations were performed with the HySS2 program (Protonic software).

## Results and Discussion

**Previous Erroneous Applications of Standard Scatchard Plots to Multicomponent Assemblies.** Contrary to a strictly successive intermolecular binding of metal ions to a single ligand, the self-assembly of double-[15,16] or triple-stranded[2,17,18] helicates involves intra- and intermolecular processes.[18−20] Indeed, metallic complexes containing different number of ligands, denoted as $[M_mL_1]$, $[M_mL_2]$, ... $[M_mL_n]$, can be formed and their molar fractions vary with $[M]_{tot}$. However, $[L]_{tot}$ remains constant and the occupancy $r$ can be expressed as moles of bound M per mole of L.[12] It leads to eq 5, which differs from eqs 3 and 4 for the explicit consideration of the number of ligands in each complex for calculating $[L]_{tot}$ (denominator of eq 5).

$$r = \frac{[M]_{bound}}{[L]_{tot}} = \frac{\sum_m m\beta_{mn}[M]^m[L]^{n-1}}{1 + \sum_m n\beta_{mn}[M]^m[L]^{n-1}} \qquad (5)$$

For instance, when a maximum of three metals ($m_{max} = 3$) are bound to 2 ligands ($n_{max} = 2$) in trimetallic double-stranded helicates,[15,16] or to three ligands ($n_{max} = 3$) in triple-stranded helicates,[17] the values of $r$ should converge to $r_{max} = m_{max}/n_{max} = 1.5$ and 1.0, respectively. To test cooperativity for the successive metal binding in species specifically containing the aggregated receptor $L_n$, the authors[15−17] arbitrarily neglect the formation of other complexes. $[L_n]_{tot}$ is then simply approximated as $[L_n]_{tot} = [L]_{tot}/n$. Equation 5 then transforms into eq 6, and the total number of accessible sites corresponds to $r_{max} = m_{max} = 3$ (eq 6).

$$r = \frac{[M]_{bound}}{[L_n]_{tot}} = n\frac{[M]_{bound}}{[L]_{tot}} = \frac{n([M]_{tot} - [M])}{[L]_{tot}} = \frac{n\sum_m m\beta_{mn}[M]^m[L]^{n-1}}{1 + \sum_m n\beta_{mn}[M]^m[L]^{n-1}} \quad (6)$$

The occupancy $r$ (eq 6) has been subsequently considered[15−17] for the detection of cooperativity in the multimetallic helicates by using Scatchard plots ($r$/[L] vs $r$, Figures 3a and 7a). It is worth noting, that the occupancy $r$ in eq 6 nonlinearly depends on the concentration of a single strand [L], which is not compatible with the occupancy $r$ defined initially for a single ligand receptor with eq 3, whereby $r$ is independent of [L]. Moreover, the approximation $[L_n] = [L]_{tot}/n$ is valid only when all L is bound in complexes containing the aggregate form $L_n$. In the case of double- and triple-stranded helicates, the occupancy $r$ (eq 6) is indeed related to several different receptors ($L_1$, $L_2$, ... $L_n$). The shape of the associated Scatchard plot ($r$/[M] vs $r$) can be thus unraveled by analyzing eq 6. When $[M]_{tot}$ is small, the denominator of eq 6 is close to 1 because of the negligible concentration of metallic complexes $[M_mL_n]$ compared with free [L] ($1 \gg \sum_m n\beta_{mn}[M]^m[L]^{n-1}$). Therefore, a slight initial increase of $[M]_{tot}$ responsible for metal complexation causes a considerable increase of the initial occupancy $r$, referring mainly to $L_1$, and the slope of the Scatchard plot is positive ($d(r/[M])/dr > 0$). For larger amounts of $[M]_{tot}$, the complexed forms of L (i.e., $[M_mL_n]$) prevail ([L] → 0), and the denominator becomes greater than 1 ($1 \ll \sum_m n\beta_{mn}[M]^m[L]^{n-1}$). The occupancy $r$ now mainly refers to $L_n$. The slope of the Scatchard plot becomes negative ($d(r/[M])/dr < 0$), which determines the overall concave shape of the curve.

This virtual preassembling of ligands to give $L_1$, $L_2$, ... $L_n$ can be compared with the polymerization of monomeric receptors observed in biological systems,[21] which leads to an increased receptor density and therefore to an enhanced binding affinity. The formation of such receptors $L_n$, where $[L_n]$ is a function of $[L]^n$, strongly influences the curvature of the Scatchard plots. In that case, cooperativity tests can lead to misleading conclusions, as found for double- and triple-stranded helicates.[15−17] The global occupancy $r$ represented by eqs 5 or 6 can be hardly used to reasonably evaluate cooperativity in supramolecular systems, where the formation of polymetallic complexes simultaneously occurs with several receptors $L_n$.

**Adaptation of Scatchard plots to Multicomponent Assemblies: Theory of Partial Occupancy Plots for Preassembled Receptors.** As discussed previously for metal−ligand systems, reliable Scatchard plots can be constructed only when several metal ions are successively bound to a single ligand according to virtual intermolecular processes (eqs 3 and 4).[1] When several ligands are involved, the latter special situation can be induced by the use of an external linker A (for instance a metal ion,[15,22] hydrogen bonds,[23] or reversible imines[24]), which is able to connect $n$ independent binding units to give $AL_n$. The successive binding of metallic cations to the single receptor $AL_n$ then obeys the rule of strict intermolecular connection, and a partial occupancy $r_{AL_n}$, adapted to Scatchard plots, can be derived according to the following strategy. The formation of a noncovalent receptor $AL_n$ can be defined with equilibrium (eq 7), whereby A denotes the connecting agent. The subsequent metal binding to this receptor occurs according to eq 8.

$$nL + A \rightleftharpoons AL_n \quad \beta_{AL_n} = \frac{[AL_n]}{[A][L]^n} \quad (7)$$

$$mM + AL_n \rightleftharpoons M_mAL_n \quad \beta_{M_mAL_n} = \frac{[M_mAL_n]}{[AL_n][M]^m} \quad (8)$$

Usually, only the global stability constants related to the free concentrations of all components are experimentally accessible (eq 9).

$$mM + A + nL \rightleftharpoons M_mAL_n \quad \beta^{exp}_{M_mAL_n} = \frac{[M_mAL_n]}{[M]^m[A][L]^n} \quad (9)$$

The combination of eqs 7−9 shows that $\beta_{M_mAL_n}$ can be easily deduced from $\beta^{exp}_{M_mAL_n}$ and $\beta_{AL_n}$ with $\beta_{M_mAL_n} = (\beta^{exp}_{M_mAL_n}/\beta_{AL_n})$. Moreover, the total concentrations of the receptor, ligand, and bound metals are expressed with eqs 10−12.

$$[AL_n]_{tot} = [AL_n] + \sum_m [M_mAL_n] = [AL_n](1 + \sum_m \beta_{M_mAL_n}[M]^m) \quad (10)$$

$$[L]_{tot} = [L] + n[AL_n]_{tot} = [L] + n[AL_n](1 + \sum_m \beta_{M_mAL_n}[M]^m) \quad (11)$$

$$[M]^{AL_n}_{bound} = \sum_m m[M_mAL_n] = [AL_n]\sum_m m\beta_{M_mAL_n}[M]^m \quad (12)$$

By analogy to similar complexation processes involving a single ligand (eq 2), the metal binding to the preassembled receptor $AL_n$ is described by the partition function $Q_{AL_n}$ (eq 13), which represents the sum of concentrations of all species containing $AL_n$ related to the free $AL_n$.

$$Q_{AL_n} = \frac{[AL_n]_{tot}}{[AL_n]} = \frac{[AL_n] + [M_1AL_n] + ... + [M_mAL_n]}{[AL_n]} = 1 + \sum_m \beta_{M_mAL_n}[M]^m \quad (13)$$

Similarly to eq 3 for a single polytopic ligand, the desired partial occupancy factor $r_{AL_n}$ can be obtained by differentiation to give eq 14.[12] Note that $r_{AL_n}$ is independent of [L].

$$r_{AL_n} = \frac{\partial \ln Q_{AL_n}}{\partial \ln[M]} = \frac{[M]^{AL_n}_{bound}}{[AL_n]_{tot}} = \frac{\sum_m m[M_mAL_n]}{[AL_n] + \sum_m [M_mAL_n]} = \frac{\sum_m m\beta_{M_mAL_n}[M]^m}{1 + \sum_m \beta_{M_mAL_n}[M]^m} \quad (14)$$

In this context, the plot $r_{AL_n}/[M]$ vs $r_{AL_n}$ (Scatchard-like plot) corresponds to a standard Scatchard plot, but is limited to the preassembled receptor $AL_n$. Its interpretation in terms of cooperativity is the same as for the classical Scatchard plot, i.e., a concave curve is a sign of positive cooperativity, while a convex curve indicates negative cooperativity. Obviously, eq 14 can be applied for more complex systems containing several

receptors $AL_n$ with different number of connected ligands ($n$). As judiciously noticed by Ercolani,[1] only virtually identical processes can be compared to access cooperativity, which is in complete agreement with the present concept based on the calculation of $r_{AL_n}$. Considering the preassembled receptor $AL_n$, the initial metal binding reaction holds for a reference, and the sign of cooperativity of the subsequent metal binding can be judged according to the shape of the Scatchard-like plot. In other words, deviations from the repetitive statistical binding[1,6] can be detected only for the second (or higher) complexation process. For the sake of clarity, the influence of the experimental errors in stability constants on cooperativity is not discussed in this contribution.

**Application of Partial Occupancy Plots for Preassembled Receptors in Lehn's Double-Stranded Helicates.** The application of the partial occupancy concept related to a preassembled receptor $AL_n$ can be demonstrated for the complexation of L3 with Cu(I) (Scheme 1).[15] In agreement with theoretical considerations, the required preassembled noncovalent receptor $AL_2$ can be defined as the assembly of two ligands L3 with a linker A = $Cu^+$, according to eq 15. The subsequent connections of Cu(I) to $[Cu(L3)_2]^+$ are described by eqs 16 and 17, whereby the corresponding stability constants $\beta_{Cu_m(L3)_2}$ can be estimated by using the experimental values of $\beta^{exp}_{Cu_m(L3)_2}$.

$$Cu^+ + 2\,L3 \rightleftharpoons [Cu(L3)_2]^+ \quad \beta_{Cu(L3)_2} = \frac{[Cu(L3)_2]}{[Cu][L3]^2} = \beta^{exp}_{Cu(L3)_2} \tag{15}$$

$$Cu^+ + [Cu(L3)_2]^+ \rightleftharpoons [Cu_2(L3)_2]^{2+}$$

$$\beta_{Cu_2(L3)_2} = \frac{[Cu_2(L3)_2]}{[Cu][Cu(L3)_2]} = \frac{\beta^{exp}_{Cu_2(L3)_2}}{\beta_{Cu(L3)_2}} \tag{16}$$

$$2Cu^+ + [Cu(L3)_2]^+ \rightleftharpoons [Cu_3(L3)_2]^{3+}$$

$$\beta_{Cu_3(L3)_2} = \frac{[Cu_3(L3)_2]}{[Cu]^2[Cu(L3)_2]} = \frac{\beta^{exp}_{Cu_3(L3)_2}}{\beta_{Cu(L3)_2}} \tag{17}$$

In other words, the receptor $[Cu(L3)_2]^+$ is able to successively accommodate two Cu(I) cations according to eqs 18 and 19, which indeed correspond to comparable intermolecular processes.

$$Cu^+ + [Cu(L3)_2]^+ \rightleftharpoons [Cu_2(L3)_2]^{2+} \quad K_1^{Cu(L3)_2} = \beta_{Cu_2(L3)_2} \tag{18}$$

$$Cu^+ + [Cu_2(L3)_2]^{2+} \rightleftharpoons [Cu_3(L3)_2]^{3+} \quad K_2^{Cu(L3)_2} = \frac{\beta_{Cu_3(L3)_2}}{\beta_{Cu_2(L3)_2}} \tag{19}$$

The distribution of all species as a function of $[Cu(I)]_{tot}$ is calculated with the global stability constants $\beta^{exp}_{Cu_m(L3)_2}$ (the formation of $[Cu(L3)]^+$ is neglected, as in the original application of the Scatchard plot).[15] The partial occupancy $r_{Cu(L3)_2}$ related to the monometallic complex $[Cu(L3)_2]^+$ is thus calculated using eq 14, whereby $AL_n = [Cu(L3)_2]^+$. The resulting Scatchard-like plot in Figure 2 interestingly shows a downward concave curvature, which indicates positive cooperativity for the binding of the second Cu(I) to the receptor $[Cu(L3)_2]^+$ to give $[Cu_3(L3)_2]^{3+}$ (eq 19), with respect to the first one leading to $[Cu_2(L3)_2]^{2+}$ (eq 18).

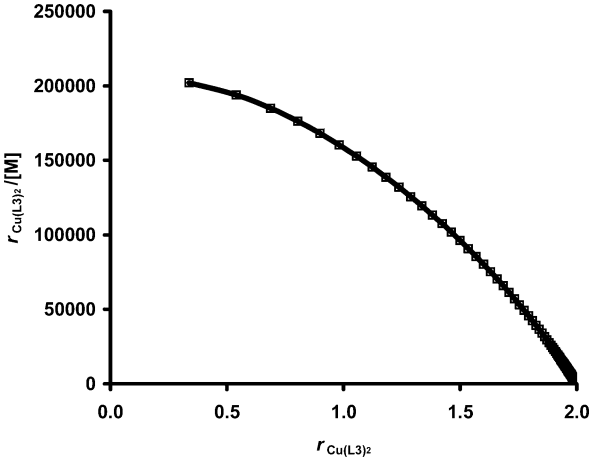


**Figure 2.** Scatchard-like plot for the binding of Cu(I) to the noncovalent receptor $[Cu(L3)_2]^+$. $[L3]_{tot} = 1 \times 10^{-4}$ M; $[Cu(I)]_{tot}$ vary between 0 and $6 \times 10^{-4}$ M. Species concentrations were calculated with $\log \beta^{exp}_{Cu(L3)_2} = 8.2$, $\log \beta^{exp}_{Cu_2(L3)_2} = 13.5$, $\log \beta^{exp}_{Cu_3(L3)_2} = 18.6$.[15]

This unexpected positive deviation from statistics could be interpreted in terms of an increased preorganization of binding sites within the receptor $[Cu(L3)_2]^+$ upon the successive complexation of two Cu(I) cations, which partially compensates the unavoidable electrostatic intermetallic repulsions. This observation is in agreement with a classical cooperativity test, which directly compares the successive stability constants. The ratio $K_2^{Cu(L3)_2}/K_1^{Cu(L3)_2} = 0.63$, which is larger than the statistical criterion 0.25. The latter value being obtained with the reasonable hypothesis that the two sites are equivalent.

**Extension of Partial Occupancy Plots for Preassembled Receptors $L_n$ without Connector.** The partial occupancy concept, developed above for a noncovalent receptor $AL_n$, in which $n$ binding units L are preassembled by a linker A, can be extended for virtual receptors $L_n$ obtained by the simple association of $n$ ligands in absence of the linker A, according to equilibrium (eq 20).

$$nL \rightleftharpoons L_n \quad \beta_{L_n} \tag{20}$$

The equilibrium constant for the formation of $L_n$ can be expressed as $\beta_{L_n} = ([L_n]/[L]^n)$. In the presence of a metal M, various complexes can be formed with $L_1$, $L_2$, ..., $L_n$. The corresponding stability constants are defined by equilibria (eqs 21−23).

$$mM + L_1 \rightleftharpoons M_mL_1 \quad \beta_{m1} = \frac{[M_mL_1]}{[M]^m[L_1]} \tag{21}$$

$$mM + L_2 \rightleftharpoons M_mL_2 \quad \beta_{m2} = \frac{[M_mL_2]}{[M]^m[L_2]} \tag{22}$$

$$\vdots$$

$$mM + L_n \rightleftharpoons M_mL_n \quad \beta_{mn} = \frac{[M_mL_n]}{[M]^m[L_n]} \tag{23}$$

However, the experimental stability constants are defined with respect to the concentration of the free ligand L, according to eq 24.

$$mM + nL \rightleftharpoons M_mL_n \quad \beta^{exp}_{mn} = \frac{[M_mL_n]}{[M]^m[L]^n} \tag{24}$$

To find the relation between the constants $\beta_{mn}$ and $\beta_{mn}^{exp}$, the substitution $[L_n] = \beta_{L_n}[L]^n$ is introduced in eqs 21−23, this leading to $\beta_{mn} = (\beta_{mn}^{exp}/\beta_{L_n})$. Obviously, $\beta_{m1}$ for the receptor $L_1$ is equal to $\beta_{m1}^{exp}$ ($L_1 = L$, $\beta_{L_1} = 1$), while $\beta_{mn} = (\beta_{mn}^{exp}/\beta_{L_n})$ holds for $L_n$. Considering equilibria eqs 21−23, the total concentrations of the different receptors are given by eqs 25−27, which can be combined to give the total concentration of the ligand in eq 28. The total concentrations of metal ions bound to each receptor are summarized by eqs 29−31.

$$[L_1]_{tot} = [L_1] + \sum_m [M_mL_1] = [L_1]\,(1 + \sum_m \beta_{m1}[M]^m) \quad (25)$$

$$[L_2]_{tot} = [L_2] + \sum_m [M_mL_2] = [L_2]\,(1 + \sum_m \beta_{m2}[M]^m) \quad (26)$$

$$\vdots$$

$$[L_n]_{tot} = [L_n] + \sum_m [M_mL_n] = [L_n]\,(1 + \sum_m \beta_{mn}[M]^m) \quad (27)$$

$$[L]_{tot} = [L_1]_{tot} + 2[L_2]_{tot} + \ldots + n[L_n]_{tot}$$
$$= [L_1]\,(1 + \sum_m \beta_{m1}[M]^m) + 2[L_2]\,(1 + \sum_m \beta_{m2}[M]^m) + \ldots + n[L_n]\,(1 + \sum_m \beta_{mn}[M]^m) \quad (28)$$

$$[M]_{bound}^{L_1} = \sum_m m[M_mL_1] = [L_1]\sum_m m\beta_{m1}[M]^m \quad (29)$$

$$[M]_{bound}^{L_2} = \sum_m m[M_mL_2] = [L_2]\sum_m m\beta_{m2}[M]^m \quad (30)$$

$$\vdots$$

$$[M]_{bound}^{L_n} = \sum_m m[M_mL_n] = [L_n]\sum_m m\beta_{mn}[M]^m \quad (31)$$

Similarly to a noncovalent receptor (eq 13), metal binding reactions to each preassembled receptor $L_n$ are described by the partition functions (eqs 32−34), which correspond to the sum of concentrations of all species in a specific family (Scheme 2) relative to the free receptors.

$$Q_{L_1} = \frac{[L_1]_{tot}}{[L_1]} = 1 + \sum_m \beta_{m1}[M]^m \quad (32)$$

$$Q_{L_2} = \frac{[L_2]_{tot}}{[L_2]} = 1 + \sum_m \beta_{m2}[M]^m \quad (33)$$

$$\vdots$$

$$Q_{L_n} = \frac{[L_n]_{tot}}{[L_n]} = 1 + \sum_m \beta_{mn}[M]^m \quad (34)$$

The partial occupancy factors $r_{L_n}$ we are looking for can be obtained by differentiation of the ln $Q_{L_n}$ with respect to ln [M] (eqs 32−34), leading to the general eq 35.[12] The related plots $r_{L_n}$/[M] vs $r_{L_n}$ correspond to Scatchard-like plots for the receptors $L_n$.

$$r_{L_n} = \frac{\partial \ln Q_{L_n}}{\partial \ln[M]} = \frac{\sum_m m\beta_{mn}[M]^m}{1 + \sum_m \beta_{mn}[M]^m} = \frac{[M]_{bound}^{L_n}}{[L_n]_{tot}} \quad (35)$$

**SCHEME 2: Equilibria between Distinct Groups of Species Related to $L_n$. Only Apparent General Equilibrium Constants $\beta'_{L_n}$ (eq 36) Are Shown for Clarity**

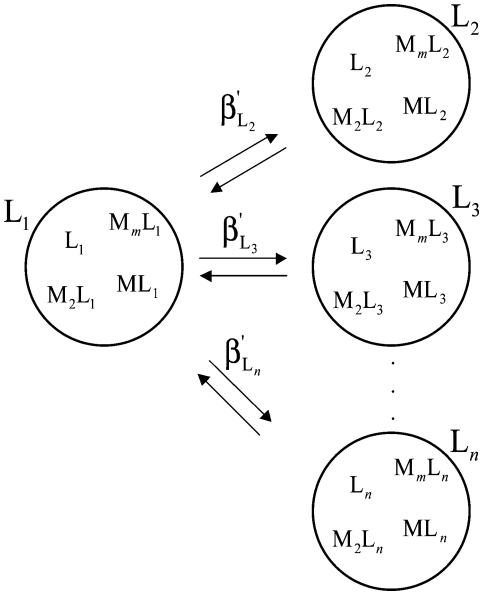


Finally, solution equilibria between distinct groups of species (i.e. $M_mL_1$ and $M_mL_n$, $m = 0, 1, \ldots$) can be characterized by the apparent general equilibrium constant $\beta'_{L_n}$ (eq 36, Scheme 2). This relation allows to calculate the distribution of species containing different receptors $L_n$ under various experimental conditions.[12]

$$\beta'_{L_n} = \frac{[L_n]_{tot}}{([L_1]_{tot})^n} = \frac{[L_n]\,(1 + \sum_m \beta_{mn}[M]^m)}{[L_1]^n\,(1 + \sum_m \beta_{m1}[M]^m)^n} = \beta_{L_n}\frac{1 + \sum_m \beta_{mn}[M]^m}{(1 + \sum_m \beta_{m1}[M]^m)^n} \quad (36)$$

In diluted solutions, almost no aggregation of ligands to form $L_n$ is experimentally detected. In other words, the free concentration $[L_n]$ ($[L_n] = \beta_{L_n}[L]^n$) is negligible compared with the concentration of the metallic complexes $[M_mL_n]$. This assumption implies that $[L_n] \ll \sum_m \beta_{mn}[M]^m[L_n]$ for all $[M]_{tot}$, so $1 \ll \sum_m \beta_{mn}[M]^m$ in the denominator of eq 35, which eventually reduces to eq 37.

$$r_{L_n} = \frac{[M]_{bound}^{L_n}}{[L_n]_{tot}} = \frac{\sum_m m\beta_{mn}[M]^m}{\sum_m \beta_{mn}[M]^m} = \frac{\sum_m m\beta_{mn}^{exp}[M]^m}{\sum_m \beta_{mn}^{exp}[M]^m} \quad (37)$$

Since the preorganization of $L_n$ affects similarly all complexes, $\beta_{L_n}$ can be put in evidence and $\beta_{mn}$ can be simply replaced by $\beta_{mn}^{exp}$ (eq 37). Concerning the absolute value of $\beta_{L_n}$, which is usually not determined, a small value is expected to justify a negligible concentration of $L_n$ ($[L_n] \rightarrow 0$). It is worth noting that in the site-binding model,[2,3,6] the free energy associated with the receptor formation $\Delta G_{L_n} = -RT \ln \beta_{L_n}$ (mainly entropic contributions) is considered as a fixed translation of the zero-level of the free energy scale, which is arbitrarily

set to zero ($\Delta G_{L_n} = 0 \rightarrow \beta_{L_n} = 1$). If this assumption ($\beta_{L_n} = 1$) is adopted for $L_n$, $\beta_{mn} = \beta_{mn}^{exp}$ and eq 35 again reduces to eq 37.

**Application of Partial Occupancy Plots for Preassembled Receptors $L_n$ in Lehn's Double-Stranded Helicates.** The formation of Lehn's archetypal Cu(I) double-stranded helicates with L3, to eventually give $[Cu_3(L3)_2]^{3+}$,[15] represents a classical example for the evaluation of homotropic cooperativity. According to our extended model considering preassembled receptors $L_n$, the complete system of stability constants related to the different receptors (L3) and $(L3)_2$ can be described with eqs 38−42:

$$2\,L3 \rightleftharpoons (L3)_2 \quad \beta_{(L3)_2} = \frac{[(L3)_2]}{[(L3)]^2} \tag{38}$$

$$Cu^+ + L3 \rightleftharpoons [Cu(L3)]^+ \quad \beta_{Cu(L3)} = \frac{[Cu(L3)]}{[Cu][(L3)]} = \beta_{Cu(L3)}^{exp} \tag{39}$$

$$Cu^+ + (L3)_2 \rightleftharpoons [Cu(L3)_2]^+$$

$$\beta_{Cu(L3)_2} = \frac{[Cu(L3)_2]}{[Cu][(L3)_2]} = \frac{\beta_{Cu(L3)_2}^{exp}}{\beta_{(L3)_2}} \tag{40}$$

$$2Cu^+ + (L3)_2 \rightleftharpoons [Cu_2(L3)_2]^{2+}$$

$$\beta_{Cu_2(L3)_2} = \frac{[Cu_2(L3)_2]}{[Cu]^2[(L3)_2]} = \frac{\beta_{Cu_2(L3)_2}^{exp}}{\beta_{(L3)_2}} \tag{41}$$

$$3Cu^+ + (L3)_2 \rightleftharpoons [Cu_3(L3)_2]^{3+}$$

$$\beta_{Cu_3(L3)_2} = \frac{[Cu_3(L3)_2]}{[Cu]^3[(L3)_2]} = \frac{\beta_{Cu_3(L3)_2}^{exp}}{\beta_{(L3)_2}} \tag{42}$$

Due to the presence of the same bipyridine binding units along the ligand strands, all coordination sites in the receptor $(L3)_2$ are considered to be equivalent, and each metal is bound in the same way. In the original paper,[15] the formation of $[Cu(L3)]^+$ is not taken into account for the calculation of cooperativity. For the sake of comparison, this complex will be also neglected in our initial rough analysis. The presence of $[(L3)_2]$ has not been experimentally detected, and the partial occupancy $r_{(L3)_2}$ is then calculated according to eq 37, where the concentrations of Cu(I) complexed with $(L3)_2$ {$[Cu(L3)_2]^+$, $[Cu_2(L3)_2]^{2+}$, and $[Cu_3(L3)_2]^{3+}$} are computed using their experimental formation constants $\beta_{mn}^{exp}$ determined by Lehn at al.[15]

The corresponding Scatchard-like plot is given in Figure 3b. The curve begins around $r_{(L3)_2} = m_{min} = 1$, which means, that the initially added metal is quantitatively complexed by $(L3)_2$ (formation of $[Cu(L3)_2]^+$, eq 43).

$$Cu^+ + (L3)_2 \rightleftharpoons [Cu(L3)_2]^+ \quad K_1^{(L3)_2} = \frac{\beta_{Cu(L3)_2}^{exp}}{\beta_{(L3)_2}} \tag{43}$$

$$Cu^+ + [Cu(L3)_2]^+ \rightleftharpoons [Cu_2(L3)_2]^{2+} \quad K_2^{(L3)_2} = \frac{\beta_{Cu_2(L3)_2}^{exp}}{\beta_{Cu(L3)_2}^{exp}} \tag{44}$$

$$Cu^+ + [Cu_2(L3)_2]^{2+} \rightleftharpoons [Cu_3(L3)_2]^{3+} \quad K_3^{(L3)_2} = \frac{\beta_{Cu_3(L3)_2}^{exp}}{\beta_{Cu_2(L3)_2}^{exp}} \tag{45}$$

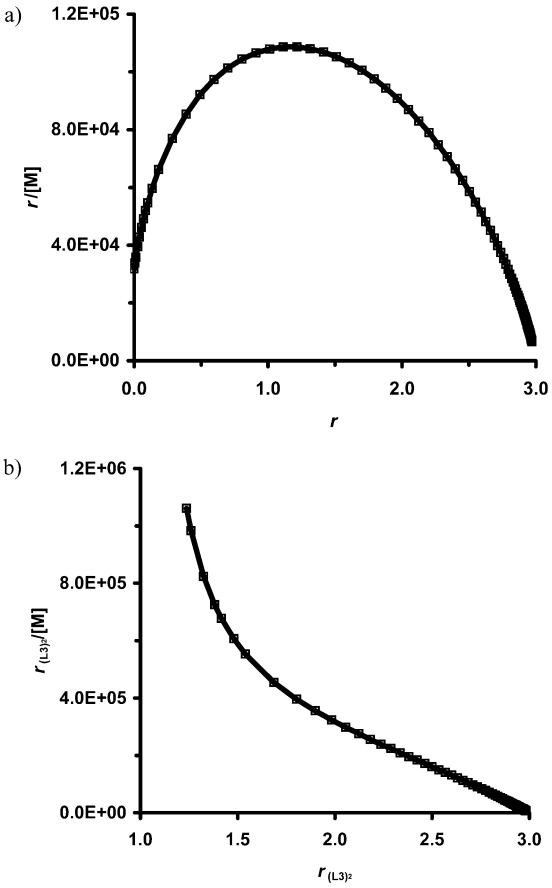


**Figure 3.** Plots for Lehn's helicates. (a) Scatchard plot (eq 6) for the formation $[Cu_3(L3)_2]^{3+}$ calculated with the stability constants determined in ref 15, except $\beta_{Cu(L3)}^{exp}$. (b) Related Scatchard-like plot using the partial occupancy given by eq 37. ($[L3]_{tot} = 1 \times 10^{-4}$ M; $[Cu(I)]_{tot}$ vary between 0 and $6 \times 10^{-4}$ M; log $\beta_{Cu(L3)_2}^{exp} = 8.2$, log $\beta_{Cu_2(L3)_2}^{exp} = 13.5$, log $\beta_{Cu_3(L3)_2}^{exp} = 18.6$).[15]

Upon increasing partial occupancy, a convex curve is observed between $r_{(L3)_2} = 1-2$, indicating a negatively cooperative binding of the second cation (eq 44) with respect to the first one. This behavior can be assigned to the electrostatic repulsions between two charged species $Cu^+$ and $[Cu(L3)_2]^+$ (contrary to $Cu^+$ binding to neutral $(L3)_2$, eq 43), and it matches the results obtained using the extended site-binding model.[5] For the binding of the third metal cation, a slightly downward concave curve is observed for $r_{(L3)_2} = 2-3$ (Figure 3b). The observed positive cooperativity is attributed to an increased preorganization of $[Cu_2(L3)_2]^{2+}$ for complexing the third cation (eq 45), as discussed previously for a noncovalent receptor $[Cu(L3)_2]^+$ (eqs 18−19). The qualitative results obtained graphically by the Scatchard-like plot are equivalent to the cooperativity tests based on the ratio of the successive stability constants $K_m^{(L3)_2}$, which are related to virtually identical intermolecular processes (equilibria 43−45). However, this test is relevant only if the stability constant $\beta_{(L3)_2}$ is known for calculating $K_1^{(L3)_2}$ (eq 43). On the other hand, the subsequent ratio $K_3^{(L3)_2}/K_2^{(L3)_2} = 0.63$ does not depend on $\beta_{(L3)_2}$. This value is larger than 1/3, the statistical value calculated for a receptor with three equivalent binding sites.[7] We deduce that the fixation of the last metal is driven by positive cooperativity, in perfect agreement with the Scatchard-like plot in Figure 3b.

A more complete treatment of the occupancy takes into account the global system including $[Cu(L3)]^+$ (eq 39). Thus, four complexes, related to two receptors, $(L3)_2$ {$[Cu(L3)_2]^+$, $[Cu_2(L3)_2]^{2+}$, $[Cu_3(L3)_2]^{3+}$}, and $(L3)_1$ {$[Cu(L3)]^+$}, exist in

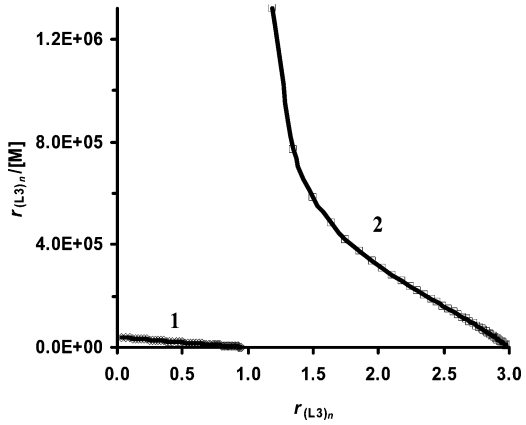


**Figure 4.** Scatchard-like plots for the formation $(L3)_1$ (**1**) and $(L3)_2$ (**2**) complexes. Calculated with the stability constants determined in ref 15 including $\beta^{exp}_{Cu(L3)}$ ($[L3]_{tot} = 1 \times 10^{-4}$ M; $[Cu(I)]_{tot}$ vary between 0 and $6 \times 10^{-4}$ M; $\log \beta^{exp}_{Cu(L3)} = 4.6$, $\log \beta^{exp}_{Cu(L3)_2} = 8.2$, $\log \beta^{exp}_{Cu_2(L3)_2} = 13.5$, $\log \beta^{exp}_{Cu_3(L3)_2} = 18.6$).

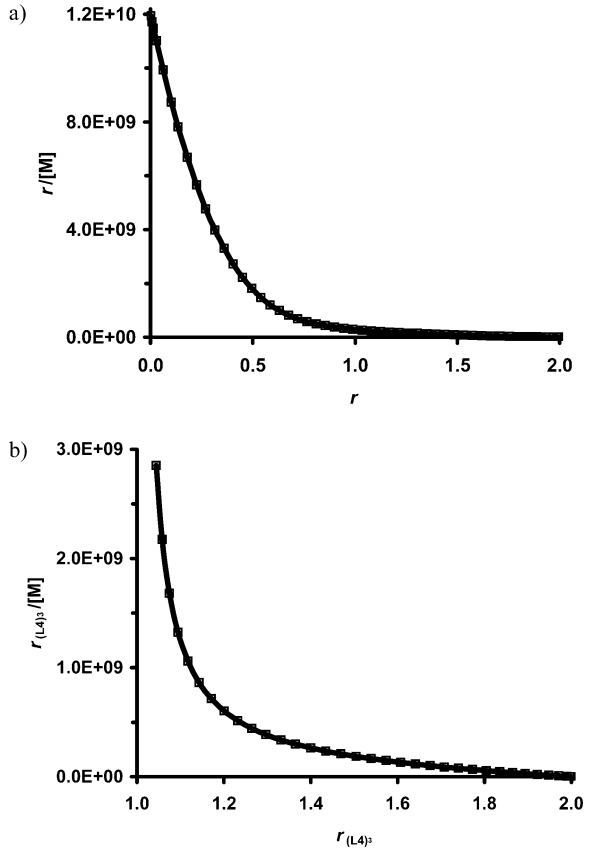


**Figure 5.** Bimetallic triple-stranded helicates with L4. (a) Unadapted Scatchard plot calculated with eq 6. (b) Reliable Scatchard-like plot with the partial occupancy given by eq 37. ($[L4]_{tot} = 2 \times 10^{-4}$ M; $[La(III)]_{tot}$ vary between 0 and $1.4 \times 10^{-4}$ M; $\log \beta^{exp}_{La(L4)_3} = 17.0$, $\log \beta^{exp}_{La_2(L4)_3} = 25.1$).[2]

solution. Their concentrations are calculated as a function of $[M]_{tot}$ by using the experimental stability constants $\beta^{exp}_{Cu_m(L3)_n}$.[15]

Equation 35 must be used in order to calculate the partial occupancy $r_{(L3)_1}$ because of the presence of [L3]. Since $[(L3)_2]$ is not experimentally observed ($[(L3)_2] \rightarrow 0$), $r_{(L3)_2}$ is computed according to eq 37. The resulting Scatchard-like plots ($r_{(L3)_n}$/[M] vs $r_{(L3)_n}$) are given in Figure 4 and indeed demonstrate that Cu(I) is mainly bound in species with $(L3)_2$ (curve 2), while species with $(L3)_1$ are less significant (curve 1). A straight line obviously results for the receptor $(L3)_1$, because a single complex $[Cu(L3)]^+$ is formed. For the receptor $(L3)_2$, the observation of a convex curve for $r_{(L3)_2} = 1-2$ followed by a slightly concave curve for $r_{(L3)_2} = 2-3$ confirms the occurrence of successive negative and positive cooperativity as discussed in the previous paragraph. Comparison with Figure 3b shows that the Scatchard-like plot for $(L3)_2$ does not significantly change when $[Cu(L3)]^+$ is explicitly considered.

**Application of Partial Occupancy Plots for Preassembled Receptors in Triple-Stranded Helicates.** The formation of bimetallic triple-stranded helicates with L4 (Scheme 1) was investigated by Zeckert at al.[2] In this system, only mono- and bimetallic complexes containing three ligands have been identified and characterized in acetonitrile for the M/L ratio 0−0.67. As an example, the global occupancy $r$ is computed for the La(III) complexes ($\log \beta^{exp}_{La(L4)_3} = 17.0$, $\log \beta^{exp}_{La_2(L4)_3} = 25.1$) according to eq 6, and the unadapted standard Scatchard plot is shown in Figure 5a. A convex curve can be taken as an apparent sign of negative cooperativity, but no definitive conclusion can be drawn because intra- and intermolecular complexation processes occur. Now, let us consider a preassembled receptor $(L4)_3$ and the related La(III) complexes, whose stability constants are described by equilibria equations 46−48.

$$3L4 \rightleftharpoons (L4)_3 \quad \beta_{(L4)_3} = \frac{[(L4)_3]}{[(L4)]^3} \tag{46}$$

$$La^{3+} + (L4)_3 \rightleftharpoons [La(L4)_3]^{3+}$$

$$\beta_{La(L4)_3} = \frac{[La(L4)_3]}{[La][(L4)_3]} = \frac{\beta^{exp}_{La(L4)_3}}{\beta_{(L4)_3}} \tag{47}$$

$$2La^{3+} + (L4)_3 \rightleftharpoons [La_2(L4)_3]^{6+}$$

$$\beta_{La_2(L4)_3} = \frac{[La_2(L4)_3]}{[La]^2[(L4)_3]} = \frac{\beta^{exp}_{La_2(L4)_3}}{\beta_{(L4)_3}} \tag{48}$$

The partial occupancy $r_{(L4)_3}$ is calculated with eq 37 since the presence of the free preorganized receptor $[(L4)_3]$ can be neglected {$(L4)_3$ is not observed in solution}. The plot $r_{(L4)_3}$/[La] vs $r_{(L4)_3}$ still results in a convex curve eventually establishing strong negative cooperativity due to the electrostatic repulsion between metallic cations within this helicate (Figure 5b). Although both calculations incidentally converge in this case to the same qualitative conclusion (negative cooperativity), only the Scatchard-like plot based on partial occupancy factors is a reliable tool to detect cooperativity.

Detailed kinetic study of Eu(III) complexes with L5 allowed the determination of stability constants $\beta_{Eu_m(L5)_n}$ for five complexes containing one {$[Eu(L5)]^+$, $[Eu_2(L5)]^{4+}$}, two {$[Eu(L5)_2]^-$, $[Eu_2(L5)_2]^{2+}$}, or three {$[Eu_2(L5)_3]$} ligands.[18] According to our model, the partial occupancy $r_{(L5)_n}$ can be calculated for two distinct families. Thus, $r_{L5}$ related to the receptor $[(L5)_1]^{2-}$ ($[L5]^{2-}$, $[Eu(L5)]^+$, $[Eu_2(L5)]^{4+}$; eqs 49−50) is obtained with eq 35 and $r_{(L5)_2}$ for the receptor $[(L5)_2]^{4-}$ ($[Eu(L5)_2]^-$, $[Eu_2(L5)_2]^{2+}$; eqs 51−53) is found with eq 37.

$$Eu^{3+} + [L5]^{2-} \rightleftharpoons [Eu(L5)]^+ \quad K_1^{L5} = \frac{[Eu(L5)]}{[Eu][L5]} = \beta^{exp}_{Eu(L5)} \tag{49}$$

$$Eu^{3+} + [Eu(L5)]^+ \rightleftharpoons [Eu_2(L5)]^{4+}$$

$$K_2^{L5} = \frac{[Eu_2(L5)]}{[Eu][Eu(L5)]} = \frac{\beta^{exp}_{Eu_2(L5)}}{\beta_{Eu(L5)}} \tag{50}$$

$$2[L5]^{2-} \rightleftharpoons [(L5)_2]^{4-} \quad \beta_{(L5)_2} = \frac{[(L5)_2]}{[(L5)]^2} \tag{51}$$

$$Eu^{3+} + [(L5)_2]^{4-} \rightleftharpoons [Eu(L5)_2]^{-}$$

$$K_1^{(L5)_2} = \frac{[Eu(L5)_2]}{[Eu][(L5)_2]} = \frac{\beta^{exp}_{Eu(L5)_2}}{\beta_{(L5)_2}} \tag{52}$$

$$Eu^{3+} + [Eu(L5)_2]^{-} \rightleftharpoons [Eu_2(L5)_2]^{2+}$$

$$K_2^{(L5)_2} = \frac{[Eu_2(L5)_2]}{[Eu][Eu(L5)_2]} = \frac{\beta^{exp}_{Eu_2(L5)_2}}{\beta_{Eu(L5)_2}} \tag{53}$$

Both Scatchard-like plots ($r_{(L5)_n}$ vs $r_{(L5)_n}$/[M], Figure 6) exhibit convex curves, which indicates strong negative cooperativity for binding of the second Eu(III) to monometallic complexes $[Eu(L5)]^+$ and $[Eu(L5)_2]^-$. As shown by us,[4] the formation of latter species is favored due to attractive interligand interactions, while intermetallic repulsions take place in bimetallic species. The same results have been obtained with the site-binding model[6] as well as with the ratio of successive stability constants, whereby $K_2^{L5}/K_1^{L5}$ for the $C_2$-symmetrical receptor L5 amounts to $6(4) \times 10^{-3} < 0.25$.[6]

Finally, equilibria 54−57 account for the formation of Piguet's trimetallic Ln(III) triple-stranded helicates with the preassembled receptor $(L6)_3$.[17]

$$3L6 \rightleftharpoons (L6)_3 \quad \beta_{(L6)_3} = \frac{[(L6)_3]}{[(L6)]^3} \tag{54}$$

$$Ln^{3+} + (L6)_3 \rightleftharpoons [Ln(L6)_3]^{3+}$$

$$\beta_{Ln(L6)_3} = \frac{[Ln(L6)_3]}{[Ln][(L6)_3]} = \frac{\beta^{exp}_{Ln(L6)_3}}{\beta_{(L6)_3}} \tag{55}$$

$$2Ln^{3+} + (L6)_3 \rightleftharpoons [Ln_2(L6)_3]^{6+}$$

$$\beta_{Ln_2(L6)_3} = \frac{[Ln_2(L6)_3]}{[Ln]^2[(L6)_3]} = \frac{\beta^{exp}_{Ln_2(L6)_3}}{\beta_{(L6)_3}} \tag{56}$$

$$3Ln^{3+} + (L6)_3 \rightleftharpoons [Ln_3(L6)_3]^{9+}$$

$$\beta_{Ln_3(L6)_3} = \frac{[Ln_3(L6)_3]}{[Ln]^3[(L6)_3]} = \frac{\beta^{exp}_{Ln_3(L6)_3}}{\beta_{(L6)_3}} \tag{57}$$

In this metal−ligand system, only the complexes $[Ln_2(L6)_3]^{6+}$ and $[Ln_3(L6)_3]^{9+}$ are observed in solution for the ratio Ln/L = 0−1 and the equilibrium constant for the initial metal binding (eq 55) is not accessible. Considering a negligible concentration of $(L6)_3$ (not experimentally detected), the partial occupancy $r_{(L6)_3}$ is computed for the La(III) complexes by using eq 37. The plot $r_{(L6)_3}$/[La] vs $r_{(L6)_3}$ (Figure 7b) results in a convex curve for $r_{(L6)_3} = 2-3$, which apparently indicates negative cooperativity.

Due to the high stability constant ($\log \beta^{exp}_{La_2(L6)_3} = 25.0$), two La(III) cations are initially bound in $[La_2(L6)_3]^{6+}$ and $[(L6)_3] \ll [La_2(L6)_3]^{6+}$. Consequently, the initial partial occupancy amounts to $r_{(L6)_3} \cong 2$. Further decreasing of $r_{(L6)_3}$/[La] with increasing $[La]_{tot}$ refers to the fixation of the third lanthanide to $[La_2(L6)_3]^{6+}$ to form $[La_3(L6)_3]^{9+}$ ($\log \beta^{exp}_{La_3(L6)_3} = 34.3$). However, this final metallic binding is not comparable with the previous formation of the bimetallic assembly, since the successive constants are not related to the same virtual processes. Therefore, any reasonable conclusion concerning cooperativity cannot be drawn for this self-assembly, where one successive stability constant is missing. Similar analysis and conclusions hold for Lehn's Ag(I) double-stranded helicates,[16] where the stability constants have been also determined only for bi- and trimetallic complexes.

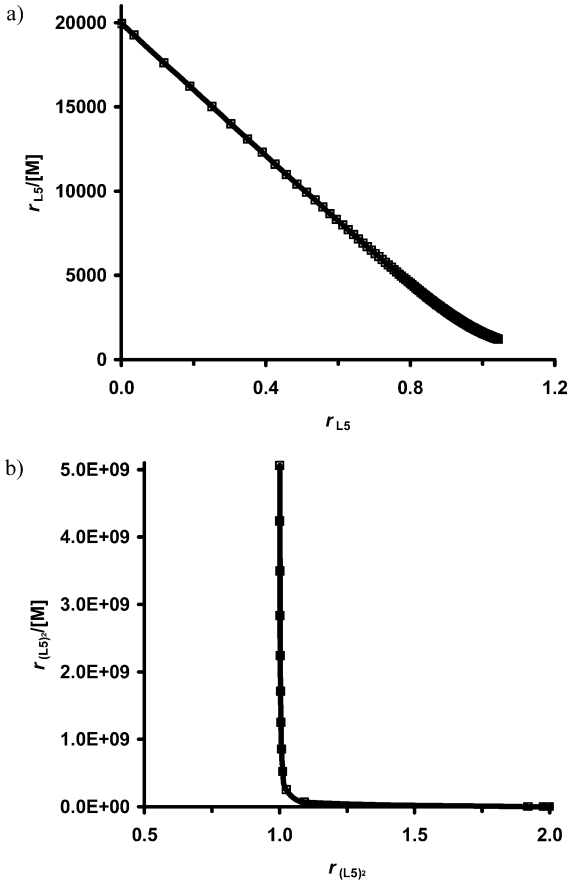


**Figure 6.** Bimetallic triple-stranded helicates with L5. Scatchard-like plots with the partial occupancy given (a) by eq 35 for L5 and (b) by eq 37 for $(L5)_2$ ($[L5]_{tot} = 2 \times 10^{-4}$ M; $[Eu(III)]_{tot}$ vary between 0 and $1 \times 10^{-3}$ M).[18]

## Conclusion

Recently developed thermodynamic models point out statistical or negative cooperativity for the formation of multimetallic helicates with neutral ligands, which is in contrast with the claim for positive cooperativity proposed in original papers, whereby Scatchard plots were used. Whereas the classical Scatchard plot operates with the global occupancy $r$ for a single ligand L, we introduce the partial occupancy $r_{AL_n}$ related to a single receptor $AL_n$ made up of $n$ ligands noncovalently linked by a connector A. This new concept allows to reliably evaluate the cooperative interactions within distinct groups of polymetallic complexes $M_mAL_n$ containing the receptor $AL_n$, whose stability constant is experimentally accessible. This approach is easily extended for receptors $L_n$ without linker. Usually, these receptors are only present in the form of metallic complexes, and the concentration of the free receptor $L_n$ cannot be experimentally detected and can be neglected. The application of partial occupancy factors is illustrated and discussed for several polymetallic helicates. The interpretation of the Scatchard-like plots ($r_{AL_n}$/[M] vs $r_{AL_n}$, $r_{L_n}$/[M] vs $r_{L_n}$) indeed agrees with recent thermodynamic models, which validates the use of this simple graphical qualitative tool

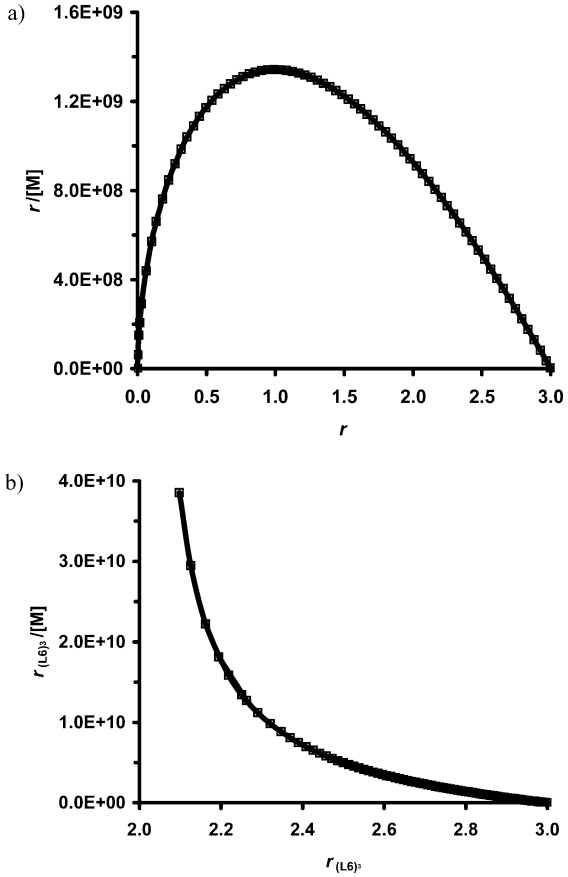


**Figure 7.** Piguet's triple-stranded helicates. (a) Unadapted Scatchard plot (eq 6) for the formation of $[La_3(L6)_3]^{9+}$. (b) Scatchard-like plot with the occupancy given by eq 37 ($[L6]_{tot} = 2 \times 10^{-4}$ M; $[La(III)]_{tot}$ vary between 0 and $2 \times 10^{-4}$ M; $\log \beta^{exp}_{La_2(L6)_3} = 25.0$, $\log \beta^{exp}_{La_3(L6)_3} = 34.3$).[17]

for other multicomponent assemblies. This approach is particularly suited for a detection of cooperativity in metal−ligand systems matching the site-binding model. Advantageously, such kind of graphical plots easily provides qualitative information about cooperative or noncooperative interactions within the self-assembly without relying to sophisticated thermodynamic modeling. However, one should always keep in mind, that only virtually identical processes can be compared in a reliable interpretation of Scatchard or Scatchard-like plots.

**Acknowledgment.** This work was supported through grants from the Swiss National Science Foundation and COST D31.

## References and Notes

(1) Ercolani, G. *J. Am. Chem. Soc.* **2003**, *125*, 16097.

(2) Zeckert, K.; Hamacek, J.; Rivera, J.-P.; Floquet, S.; Pinto, A.; Borkovec, M.; Piguet, C. *J. Am. Chem. Soc.* **2004**, *126*, 11589.

(3) Borkovec, M.; Hamacek, J.; Piguet, C. *J. Chem. Soc., Dalton Trans.* **2004**, 4096.

(4) Hamacek, J.; Borkovec, M.; Piguet, C. *Chem. Eur. J.* **2005**, *11*, 5217.

(5) Hamacek, J.; Borkovec, M.; Piguet, C. *Chem. Eur. J.* **2005**, *11*, 5227.

(6) Piguet, C.; Borkovec, M.; Hamacek, J.; Zeckert, K. *Coord. Chem. Rev.* **2005**, *249*, 705.

(7) Perlmutter-Hayman, B. *Acc. Chem. Res.* **1986**, *19*, 90.

(8) Scatchard, G. *Ann. N. Y. Acad. Sci.* **1949**, *51*, 660.

(9) Yatsimirsky, A. K. In *Encyclopedia of Supramolecular Chemistry*; Atwood, J. L., Steed, J. W., Eds.; Marcel Dekker: New York, 2004; p 20.

(10) Gibson, H. W.; Yamaguchi, N.; Hamilton, L.; Jones, J. W. *J. Am. Chem. Soc.* **2002**, *124*, 4653.

(11) (a) Rydberg, J. *Acta Chem. Scand.* **1961**, *15*, 1723. (b) Martell, A. E.; Smith, R. M. *Critical Stability Constants*; Plenum: New York, 1982; Vols. 4, 5.

(12) Wyman, J.; Gill, S. J. *Binding and Linkage, Functional Chemistry of Biological Macromolecules*; University Science Books: Mill Valley, CA 1990.

(13) Rebek, J., Jr.; Costello, T.; Marshall, L.; Wattley, R.; Gadwood, R. C.; Onan, K. *J. Am. Chem. Soc.* **1985**, *107*, 7481.

(14) Blanc, S.; Yakirevich, P.; Leize, E.; Meyer, M.; Libman, J.; Van Dorsselaer, A.; Albrecht-Gary, A.-M.; Shanzer, A. *J. Am. Chem. Soc.* **1997**, *119*, 4934.

(15) Pfeil, A.; Lehn, J.-M. *J. Chem. Soc., Chem. Commun.* **1992**, 838.

(16) Garrett, T. M.; Koert, U.; Lehn, J.-M. *J. Phys. Org. Chem.* **1992**, *5*, 529.

(17) Floquet, S.; Ouali, N.; Bocquet, B.; Bernardinelli, G.; Imbert, D.; Bünzli, J.-C. G.; Hopfgartner, G.; Piguet, C. *Chem. Eur. J.* **2003**, *9*, 1860.

(18) Elhabiri, M.; Hamacek, J.; Bünzli, J.-C. G.; Albrecht-Gary, A. M. *Eur. J. Inorg. Chem.* **2004**, 51.

(19) Fatin-Rouge, N.; Blanc, S.; Pfeil, A.; Rigault, A.; Albrecht-Gary, A. M.; Lehn, J.-M. *Helv. Chim. Acta* **2001**, *84*, 1694.

(20) Hamacek, J.; Blanc, S.; Elhabiri, M.; Leize, E.; van Dorsselaer, A.; Piguet, C.; Albrecht-Gary, A. M. *J. Am. Chem. Soc.* **2003**, *125*, 1541.

(21) Chamberlin, S. G.; Davies, D. E. *Biochim. Biophys. Acta* **1998**, *1384*, 223.

(22) (a) Rigault, S.; Piguet, C.; Bernardinelli, G.; Hopfgartner, G. *Angew. Chem., Int. Ed. Engl.* **1998**, *37*, 169. (b) Cantuel, M.; Bernardinelli, G.; Imbert, D.; Bünzli, J.-C. G.; Hopfgartner, G.; Piguet, C. *J. Chem. Soc., Dalton Trans.* **2002**, 1929.

(23) Telfer, S. G.; Kuroda, R. *Chem. Eur. J.* **2005**, *11*, 57.

(24) (a) Nitschke, J. *Angew. Chem., Int. Ed. Engl.* **2004**, *43*, 3073. (b) Schultz, D.; Nitschke, J. *Proc. Natl. Acad. Sci. U.S.A.* **2005**, *102*, 11191.